ORIGINAL ARTICLE

Investigating impacts of the mycothiazole chemotype as a chemical probe for the study of mitochondrial function and aging

Naibedya Dutta · Joe A. Gerke · Sofia F. Odron · Joseph D. Morris · Adam Hruby · Juri Kim · Toni Castro Torres · Sarah J. Shemtov · Jacqueline G. Clarke · Michelle C. Chang · Hooriya Shaghasi · Marissa N. Ray · Maxim Averbukh · Sally Hoang · Maria Oorloff · Athena Alcala · Matthew Vega · Hemal H. Mehta · Max A. Thorwald · Phillip Crews · Marc Vermulst · Gilberto Garcia · Tyler A. Johnson · Ryo Higuchi-Sanabria

Abstract Small molecule inhibitors of the mitochondrial electron transport chain (ETC) hold significant promise to provide valuable insights to the field of mitochondrial research and aging biology. In this study, we investigated two molecules: mycothiazole (MTZ) - from the marine sponge *C. mycofijiensis* and its more stable semisynthetic analog 8-*O*-acetylmycothiazole (8-OAc) as potent and selective chemical probes based on their high efficiency to inhibit ETC complex I function. Similar to rotenone (Rote), MTZ, a newly employed ETC complex I inhibitor, exhibited higher cytotoxicity against cancer cell lines compared to certain non-cancer cell lines. Interestingly, 8-OAc demonstrated greater selectivity for cancer cells when compared to both MTZ and Rote, which has promising potential for anticancer therapeutic development. Furthermore, in vivo experiments with these small molecules utilizing a *C. elegans* model demonstrate their unexplored potential to investigate aging studies. We observed that both molecules have the ability to induce a mitochondria-specific unfolded protein response (UPR^{MT}) pathway, that extends lifespan of worms when applied in their adult stage. We also found that these two molecules employ different pathways to extend lifespan in worms. Whereas MTZ utilizes the transcription factors ATFS-1 and HSF1, which are involved in the UPR^{MT} and heat shock response (HSR) pathways respectively, 8-OAc only required HSF1 and not ATFS-1 to mediate its effects. This observation underscores the value of applying stable, potent, and selective next generation chemical probes to elucidate an important insight into the functional roles of various protein subunits of ETC complexes and their regulatory mechanisms associated with aging.

Keywords mitochondria · aging · stress · *C. elegans* · cancer

N. Dutta · A. Hruby · J. Kim · T. C. Torres · S. J. Shemtov · M. Averbukh · S. Hoang · M. Oorloff · A. Alcala · M. Vega · H. H. Mehta · M. A. Thorwald · M. Vermulst · G. Garcia · R. Higuchi-Sanabria (✉)
Leonard Davis School of Gerontology, University of Southern California, Los Angeles, CA 90089, USA
e-mail: ryo.sanabria@usc.edu

J. A. Gerke · S. F. Odron · J. D. Morris · J. G. Clarke · M. C. Chang · H. Shaghasi · M. N. Ray · T. A. Johnson (✉)
Department of Natural Sciences & Mathematics, Dominican University of California, San Rafael, CA 94901, USA
e-mail: tyler.johnson@dominican.edu

P. Crews
Department of Chemistry & Biochemistry, University of California, Santa Cruz, Santa Cruz, CA 95064, USA

Springer

Introduction

Mitochondria are double membrane bound cellular organelles popularly recognized as the "powerhouse of the cell" for its most well-known function of cellular respiration. Respiration involves a series of protein complexes that transfer electrons from metabolic end products such as NADH and $FADH_2$ to a final electron acceptor oxygen. These redox reactions of electron transfer are coupled with the establishment of an electrochemical gradient across the inner membrane of mitochondria, which leads to the production of energy in the form of ATP [1]. Apart from energy production, mitochondria are also involved in numerous biochemical events in a cell, including signal transduction, metabolism and nutrient breakdown, stress response, immune response, regulation of reactive oxygen species, and calcium homeostasis [2, 3]. Additionally, they also play crucial roles in the regulation of cellular fate, including the control of different cell death mechanisms, such as apoptosis [4]. Moreover, maintaining mitochondrial homeostasis is extremely important to achieve optimal cellular function. This homeostatic condition is susceptible to the exposure of various intracellular or extracellular stress conditions, such as oxidative damage, protein misfolding, and mutations in mitochondrial DNA.

When exposed to stressors, cells activate a specific and complex mitochondrial stress response to maintain the integrity and restore the functionality of mitochondria. The key feature of the mitochondrial stress response is the activation of the mitochondrial unfolded protein response (UPR^MT) that includes the upregulation of genes, which encode essential proteins to restore mitochondrial homeostasis [5]. These include genes encoding mitochondria-specific chaperones and proteases to refold or clear damaged mitochondrial proteins. A growing number of studies in the last three decades have established that the combination of mitochondrial dysfunction and an ineffective mitochondrial stress response is strongly associated with the progression of aging and the onset of age-related degenerative diseases like neurodegenerative disorders, cardiovascular diseases, and metabolic disorders. These critical functions of mitochondria mark mitochondrial dysfunction as one of the 12 hallmarks of aging [6–8].

Despite the consequences of mitochondrial dysfunction, exposure to small doses of mitochondrial stress can be beneficial to an organism. While excessive or chronic mitochondrial stress leads to detrimental consequences to the cell, exposure to lower levels of stress, which can be induced by various interventions such as exercise, dietary restriction, or pharmacological agents, can actually trigger a hormetic response in mitochondria (i.e., mitohormesis) [9]. Mitohormesis involves the activation of beneficial transcriptional programs, including the UPR^MT, which improves cellular resilience to subsequent exposure to stress. Notably, several studies have also demonstrated that mitohormesis can even increase lifespan in various model organisms including *C. elegans* and *D. melanogaster* [10, 11].

Altogether, understanding mitohormesis can provide a detailed insight into how the cellular stress response pathways can be employed to promote healthspan and increase longevity. However, most models of mitohormesis including the nematode model, *C. elegans*, involve genetic perturbations of mitochondrial function [12, 13]. While these studies show robust activation of UPR^MT and significantly increased longevity upon disruption of mitochondrial function, genetic manipulation may be more limiting in higher organisms, especially in humans. As an alternative to genetic approaches, selected small molecule inhibitors isolated from natural sources have garnered considerable attention due to ease of delivery and their robust downstream effects [14]. The use of small molecule chemical probes to accelerate the understanding of mitochondrial dynamics has been substantial [15]. Surprisingly, a number of non-specific chemical probes have and continue to gain widespread use throughout the field of chemical biology [16]. Alternatively, a small but growing number of optimized chemical probes exist that are now proven to be chemically stable (>6 mo. shelf life), potent (<100 nM), and selective for their mechanism of action [17]. Marine natural products are a burgeoning source of next generation chemical probes to accelerate the study of the cytoskeleton [18], neuroscience [19], and mitochondrial dynamics [20] in biomedical research.

In this study, we sought to investigate the rarely studied, but potent marine sponge-derived natural product mycothiazole (MTZ), and its semisynthetic derivative 8-*O*-acetylmycothiazole (8-OAc) for their ability to serve as distinct chemical probes that affect the aging process. Recently MTZ was reported as a

potent cytotoxic compound against a wide range of cancer cell lines [21]. Both MTZ and 8-OAc were also reported to function as potent and selective inhibitors of the mitochondrial electron transport chain (ETC) complex I [20].

Similar to genetic interventions, we found that MTZ and 8-OAc were able to achieve a mitohormetic effect in *C. elegans* and prolong longevity in adult worms. Perhaps most surprising, we found that these compounds utilized distinct mechanisms to prolong longevity, suggesting that even compounds of the same chemotypes that have identical targets may activate different pathways as chemical probes based on subtle changes in their structural framework. In addition, we found that both compounds could preferentially target cancer cells for the initiation of cell death pathways, while having minimal effects on viability of non-cancer cells. Here, our results not only shed light on how these next generation small molecule chemical probes impact longevity in the model organism, *C. elegans,* but also provide an insight into their mode of actions in human cells.

Materials and methods

Human cell lines and maintenance

Human hepatocellular carcinoma (Huh7) and karyotypically normal human fibroblast (BJ) cells were a kind gift from Prof. Andrew Dillin's lab at UC Berkeley. Human embryonic kidney 293 (HEK293) cells and human glioblastoma (U87) cells were a kind gift from Dr. Marc Vermulst's lab at USC. Human breast cancer cell line (MCF7) were a kind gift from Dr. Berenice Benayoun's lab at USC. All cells were cultured in high glucose DMEM media (Cytiva) supplemented with 10% FBS (Cytiva), 1X Penicillin/Streptomycin (VWR Life Science), 1X non-essential amino acid (Cytiva) at 37°C along with 5% CO_2 in a humified incubator (Thermo). Cells were treated with compounds at ~70% confluency.

Cytotoxicity assay and determination of IC50 value

Cytotoxicity of cells was measured using 3-(4,5-diethylthiazol-2-yl)-2,5-diphenyltetrazolium bromide (MTT) assay. 70% confluent cells were grown in multi-well plates and treated with compounds or vehicle/DMSO for 24 h under above mentioned standard condition. Post-treatment, growth media was replaced with 0.5 mg/ml MTT solution and incubated for 4 h at 37 °C. After removing the MTT solution, formazan crystals were dissolved in DMSO and OD was measured at 570 nm using SpectraMax M2 microplate reader. To calculate the IC50 value we have plotted experimental values using a X-Y scattered plot with a straight line or linear regression equation (y=mx+C).

Apoptosis assay

Cells were grown up to ~70% confluency in a 6 well plate and treated with indicated concentration of compounds or vehicle for 24 h. Post incubation, cells were processed for apoptosis using flow cytometry according to the protocol described in FITC Annexin-V apoptosis detection kit (BD Pharmingen).

Measurement of ROS by DHE staining

After treating the cells with indicated concentration of compounds or vehicle control for 24 h growth media was replaced with 5 mM DHE solution and further incubated for 30 mins at 37 °C. ROS amount was determined by measuring the fluorescence of 2-hydroxyethidium, an oxidized product of DHE using flow cytometry.

Mitochondrial labeling using Mitotracker green dye

70% confluent Huh7 and BJ fibroblast cells, grown on 35mm glass bottom plates were treated with MTZ, 8-OAc or Rote for 24 h. Post treatment growth media was replaced with new media supplemented with 125 nM Mitotracker green solution (Thermo) and DAPI and incubated them for 30 mins at 37°C. After incubation cells were imaged using Stellaris 5 confocal microscope.

Measurement of oxygen consumption rate

Real time oxygen consumption rate was measured by using XF24/96 Extracellular flux analyzer (seahorse bioscience). For this assay, XF assay specific 96 well tissue culture plates (Provided by Agilent) were used to grow Huh7 and BJ cells. First, equal number of cells were grown directly in XF 96 well tissue culture

plates and at 70% confluency were treated with 10μM of MTZ, 8-OAc or Rote for 24 h. Post treatment cells were first washed one time with prewarmed XF real-time ATP rate assay media and replaced with 200 µl fresh media. Next the plate was placed in a 37 °C incubator not supplemented with CO_2 for 30 min. After incubation, media was removed and replaced with fresh prewarmed XF assay media to a final volume 180 µl and measurements were taken. Maximum mitochondrial respiratory capacity was estimated by further challenging the cells with 10 µM Oligomycin, 10 µM FCCP, or 5 µM Rotenone at 30, 70 and 90 minutes respectively during assay. Data was analyzed by seahorse Wave desktop software provided by Agilent.

Human cell RNAseq analysis

Huh7 and BJ fibroblast cells, cultured to 70% confluency in 6-well plates, underwent treatment with the indicated concentration of compounds or vehicle control and incubated for 24 h. Post incubation growth medium was removed, and cells were collected in 1X PBS in 1.5 ml centrifuge tubes. After a PBS wash 500 µl TRIzol was added to the cells followed by the addition of 300 µl chloroform in a heave gel phase-lock tube (VWR, 10847-802) for phase separation using centrifugation. The isolated aqueous phase, enriched with RNA, underwent purification using a standard RNA purification kit. (Quantabio, Extracta Plus 95214-050) as per manufacturer's directions.

Library preparation (mRNA library, poly A enrichment) and RNA sequencing (NovoSeq PE150. 6G raw data per sample) was performed at Novogene. Three biological replicates were measured per condition. Reads were trimmed with trim_galore-0.6.5-1 and mapped to Genome assembly: GRCh38.p14 with STAR-2.7.3a [22]. Mapped reads were counted to genes using feature Counts (Subread-2.0.0) [23] and Homo_sapiens.GRCh38.108.gtf gene annotation. Unwanted variations were removed with RUVSeq-1.32.0 [24] and differential expression analysis was performed with DESeq2-1.38.3 [25] using R-4.2.2.2.

C. *elegans* strains and maintenance

All strains used in this study are derivates of the N2 wild-type worm from the Caenorhabditis Genetics Center (CGC) and are listed in sTable 3. For maintenance of worms, animals are grown at 15 °C on OP50 *E. coli* B strain. For all experimental purposes, animals are grown at 20 °C on HT115 *E. coli* K strain bacteria unless otherwise noted. HT115 bacteria carry a pL4440 empty vector (used as a control) or pL4440 vector carrying a partial gene sequence against a specific target gene for RNAi purposes. All experiments are performed on age-matched animals synchronized using a standard bleaching protocol as previously described [5, 26]. Briefly, animals are collected from plates using M9 solution (22 mM KH_2PO_4 monobasic, 42.3 mM Na_2HPO_4, 85.6 mM NaCl, 1 mM $MgSO_4$) and bleached using a 1.8% sodium hypochlorite and 0.375 M KOH solution. Intact eggs were washed 4x with M9 solution and L1 synchronization was performed by floating eggs in M9 solution at 20 °C overnight. Synchronized L1s were grown on RNAi plates (1 mM $CaCl_2$, 5 µg/mL cholesterol, 25 mM KPO_4, 1 mM $MgSO_4$, 2% agar w/v, 0.25% Bacto-Peptone w/v, 51.3 mM NaCl, 1 µM IPTG, and 100 µg/mL carbenicillin; HT115 *E. coli* K strain containing pL4440 vector control or pL4440 with RNAi of interest). All aging experiments were performed on plates supplemented with 100 µL of 10 mg/mL FUDR spotted directly on the bacterial lawn.

For drug treatments, plates were supplemented with 1, 3, or 5 µM MTZ, 8-OAc and Rote, or an equivalent volume of DMSO. For 1 and 3 µM drug conditions, animals were placed on drug plates from L1. For 5 µM drug conditions, animals were moved onto drug plates from day 1 of adulthood; for all RNAi conditions on 5 µM drugs, L1 animals were grown on standard RNAi plates and moved onto RNAi plates containing drugs at day 1 of adulthood. For drug titration experiments, all animals were grown on all concentrations of drugs from the L1 stage and imaged when control animals reached day 1 of adulthood (3 days at 20 °C).

C. *elegans* microscopy

For all transcriptional reporter imaging (*hsp-6p::GFP, hsp-4p::GFP, hsp-16.2p::GFP*), synchronized animals were imaged at day 1 of adulthood. Animals were picked off plates and onto standard NGM plates without bacteria containing 5 µL of 100 mM sodium azide to paralyze worms. Paralyzed worms were lined up with the pharynx

facing up and imaged on a Leica M205FCA automated fluorescent stereomicroscope equipped with a standard GFP filter and Leica K5 camera and run on LAS X software. Three biological replicates were performed per experiment and one representative replicate image is shown in each figure. Detailed protocols are available at [5, 26].

C. *elegans* RNA-seq analysis

For RNA-seq experiments, germline less *glp-4(bn2)* animals were used to avoid progeny contamination and germline effects. Synchronized animals were grown on HT115 bacteria from hatch on standard RNAi plates at 22 °C until day 1 of adulthood. We opted to use 22 °C instead of the standard restrictive 25 °C for *glp-4(bn2)* animals to minimize heat-stress associated with growth at 25 °C. Importantly, after backcrossing these animals 6x to our N2 line, we found that our backcrossed *glp-4(bn2)* animals were more sensitive to elevated temperatures and exhibited full sterility at 22 °C. Animals were collected in M9 solution, M9 was replaced with 1 mL of Trizol and sample was flash-frozen in liquid nitrogen. To isolate RNA, animals were freeze/thawed 3x with liquid nitrogen with a 30 sec vortexing step between each freeze to lyse all animals. 300 μL of chloroform was added to the sample and aqueous separation of RNA was performed using centrifugation in a heave gel phase-lock tube (VWR, 10847-802). The aqueous phase was then applied to a standard RNA purification kit (Quantabio, Extracta Plus 95214-050) as per manufacturer's directions.

Library preparation (mRNA library, poly A enrichment) and RNA sequencing (NovoSeq PE150. 6G raw data per sample) was performed at Novogene. Three biological replicates were measured per condition. Reads were trimmed with trim_galore-0.6.5-1 and mapped to WBcel235 with STAR-2.7.3a [22]. Mapped reads were counted to genes using feature Counts (Subread-2.0.0) [23] and Caenorhabditis_elegans.WBcel235.107. gtf gene annotation. Unwanted variations were removed with RUVSeq-1.32.0 [24] and differential expression analysis was performed with DESeq2-1.38.3 using R-4.2.2.2 [25].

C. *elegans* lifespan

All lifespan assays were performed on standard RNAi plates with HT115 bacteria at 20 °C as previously described (Castro [27]). For drug treatments, animals were grown on RNAi plates containing 1 or 3 μM mycothiazole, 8-*O*-acteylmycothiazole, rotenone, or an equivalent volume of DMSO from the L1 stage; or animals were grown on standard RNAi plates without drug from the L1 stage and moved onto plates containing 5 μM mycothiazole, 8-*O*-acteylmycothiazole, rotenone, or an equivalent volume of DMSO at the day 1 adult stage. All animals were exposed to FUDR from the day 1 adult stage to remove eliminate progeny. The viability of animals were quantified every other day until all animals were scored as either dead or censored. Censored animals are defined as those that exhibit intestinal leakage out of the vulva, bagging (vivipary), desiccation on the walls of the petri dish, or other age-unrelated deaths. Survival curves were plotted using Prism7 software and LogRank statistical testing for calculation of p-values and a minimum of 3 biological replicates were performed for each experiment with all raw data available in sTable 4.

C. *elegans* seahorse assay

Synchronized animals were collected from plates using M9 and animals were poured onto an empty NGM plate (no bacteria). ~10-15 adults worms were pipetted off of these plates while avoiding all progeny and pipetted into each well of a Seahorse XF96 cell culture microplate. Basal oxygen consumption rate was measured using a XFe96 sensor cartridge on a Seahorse XFE96 Analyzer with 2 minutes mixing, 30 second wait, and 2 minutes measuring. Oxygen consumption rate was normalized for number of worms. For low concentration MTZ, 8-OAc, and Rote (1 and 3 μM), animals were grown on plates containing DMSO or compounds from L1 and oxygen consumption rate was measured at day 1 of adulthood. For high concentration (5 μM), animals were grown on standard NGM plates from L1 and moved onto DMSO, MTZ, 8-OAc, or Rote containing plates at day 1 of adulthood for 24 hours, and oxygen consumption rate was measured at day 2 of adulthood.

Chemical isolation of Mycothiazole (MTZ) and 8-*O*-acetylmycothiazole (8-OAc)

Biological material collection and identification: Specimens of the marine sponge *C. mycofijiensis* were collected via scuba diving in Vanuatu, as previously documented [20, 28]. Taxonomic identification was conducted by comparing characteristic biological features with reference samples from the UC Santa Cruz sponge repository. Voucher specimens and underwater photographs can be provided upon request.

Extracts of *C. mycofijiensis* were processed according to previously reported methods [21, 29, 30]. While the fat hexanes (FH) extracts are not commonly processed due to their high lipophilic content, this extract served as an enriched source of mycothiazole (MTZ) with minor amounts of the latrunculin or fijianolide (alternatively referred to as laulimalide) chemotypes. The approximate percentage of MTZ by weight in the FH, fat dichloromethane (FD), and dichloromethane methanol fat (DMMF) extract were 4.5%, 12%, and 10% respectively. All three extracts (FH, FD and DMMF) were used in the repeated scaleup HPLC isolation of pure MTZ. Pure MTZ was allocated for semi-synthesis (25.4 mg) and further biological evaluation experiments (24.9 mg).

HPLC purification was performed on a semi-preparative column (Phenomenex Inc. Luna© 5μm C18(2) 100 Å 10 × 250 mm) in conjunction with a 4.0 × 3.0 mm C18 (octadecyl) guard column and cartridge (holder part number: KJ0-4282, cartridge part number: AJ0-4287, Phenomenex Inc., Torrance, CA, USA). A reversed-phased linear gradient was employed (30:70 CH_3CN/H_2O to 80:20 over 50 minutes, ramping up to 100% CH_3CN from 51 to 61 minutes, then returning to 30:70 for re-equilibration from 62 to 73 minutes). Compound detection was measured with an Applied Biosystems 759a UV detector at a single wavelength λmax = 230 nm. For each of the extracts, MTZ would begin to elute at approximately 46 minutes. All purified compounds were dried under an N_2 gas stream, stored in amber vials, and purged with gaseous argon then sealed in a dark desiccator under vacuum.

Pure 8-*O*-acetylmycothiazole (8-OAc) was obtained by two distinct methods. The first method of acetylation employed 29.1 mg of the FH crude extract oil immersed in 1000 μL of acetic anhydride and 1000 μL of dry pyridine that were added to a reaction vial. The mixture was stirred for 24 h then quenched with 1000 μL of di-H_2O and 1000 μL of dichloromethane (DCM). The layers were inverted and allowed to separate before the DCM layer was removed from the reaction vial and dried under an N_2 gas stream. The dried DCM layer was purified using RP-HPLC (Phenomenex Luna© 5μm C18(2) 100 Å 10 × 250 mm) to yield one major fraction determined to be 9.9 mg of 8-OAc, resulting in a 34% yield. The second method of acetylation followed the same procedures but rather than reacting with the FH crude extract, purified MTZ (>95%, HPLC) was used and the amount of dry pyridine was reduced to 300 μL. This reaction with 25.4 mg of pure MTZ generated 10.9 mg of 8-OAc with a 43% yield. Notably, these acetylation reactions demonstrated higher efficiency when utilizing pure MTZ sourced from the FD crude extract. Subsequently, the purity of all compounds were confirmed to be >95% by ^1H NMR analysis using a Bruker instrument, featuring a 5 mm triple-resonance cryoprobe (^1H, ^{13}C, ^{15}N) operating at 600 MHz for ^1H experiments (Fig. s1). In total, 24.9 mg of MTZ and 20.8 mg of 8-OAc were used in the aforementioned biological evaluation experiments.

Statistical analysis

For the cell culture experiments all the individual data points combined with mean ± SD and graphs were plotted and statistically analyzed by One-way ANOVA, using GraphPad Prism 10.0. For the nematode lifespan experiments Kaplan-Meier survival graphs were plotted and the Logrank (Mantel-Cox) tests were performed using GraphPad Prism 10.0. ns = not significant, * = $p < 0.03$; ** = $p < 0.002$; *** = $p < 0.0002$; **** = $p < 0.0001$

Results

Mycothiazole and its acetylated analog show higher toxicity towards cancer cells while exhibiting mitochondrial complex I inhibition for both cancer and non-cancer cells

Utilizing MTZ and its more stable acetylated derivative 8-OAc [21], we aimed to determine the effectiveness of these two compounds against different cancer cell lines, including human hepatocellular carcinoma cells (Huh7), human glioblastoma (U87), and human breast cancer cells (MCF7) and compared these results with two human non-cancer cell types – skin fibroblast (BJ) and kidney epithelial cells (HEK293). Here, we purified MTZ from the marine sponge *C. mycofijiensis* using HPLC purification as previously reported [20, 21, 28–30]. 8-OAc was obtained by two methods: immersing fat hexane extracts and pure MTZ in acetic anhydride and dry pyridine for 24 h before the reaction was quenched with dichloromethane and di-H_2O. Purity of all compounds used in this study were confirmed to be >95% by NMR analysis (Fig. s1). In addition, we compared our results to rotenone (Rote), a classically utilized mitochondrial complex I inhibitor chemical probe as a comparative reference.

To study the biological activity of MTZ, 8-OAc, and Rote, we first determined the half-maximal inhibitory concentration (IC50) values for each compound using an MTT assay, which indirectly measures cell viability through a colorimetric assay for cell metabolic activity [10, 31]. While all three compounds display high cytotoxicity towards cancer cells, 8-OAc displays much lower cytotoxicity towards non-cancer cells compared to Rote and MTZ (Fig. 1A, Fig. s2). Since mitochondrial dysfunction is often correlated with the production of reactive oxygen species (ROS), which can lead to the initiation of apoptosis, we performed an apoptosis assay through annexin-V-FITC, and PI staining. Consistent with MTT assays, all three compounds robustly induced apoptosis in cancer cells. Although Rote showed the highest induction of apoptosis in cancer cells, Rote also induced a noticeable level of apoptosis in the non-cancer cell line, BJ fibroblasts (40-50% at 50 μM), whereas MTZ and 8-OAc failed to induce apoptosis at similar concentrations (Fig. 1B). We then directly measure the ROS production capacity of all three compounds by performing DHE staining followed by flow cytometry analysis of cells treated with all three compounds at 10 μM – a concentration that induced high levels of apoptosis in cancer cells and had minimal effects on non-cancer cells. Consistent with a role for mitochondrial-ROS in apoptosis, all three treatments induced ROS formation in Huh7 cells but had minimal effects on BJ fibroblast cells (Fig. 1C).

In an effort to more thoroughly assess the impact of these compounds on general mitochondrial function, we measured mitochondrial respiration through monitoring oxygen consumption rate by Seahorse assay. The Seahorse assay results showed that all three compounds result in a significant decrease in mitochondrial respiration in both cancer and non-cancer cells (Fig. 1D). Interestingly, although all three compounds induce significant mitochondrial dysfunction in both cancer and non-cancer cells, we found that these compounds only induced mitochondrial fragmentation in Huh7 cells without affecting mitochondrial morphology in BJ fibroblasts (Fig. s3). To further assess the general impact of these compounds on cellular health, we measured the impact of compound treatment on gene expression through RNA-seq analysis (Fig. s4). As expected, treatment of cancer cells with all three compounds resulted in significant gene expression changes in cell death, apoptosis, and cell cycle-related genes (sTable1). Perhaps most surprisingly, we failed to see any significantly differentially expressed genes when non-cancer cells are treated with the same concentration of these compounds. These data suggest that although all three compounds can robustly inhibit mitochondrial ETC function in both cancer and non-cancer cells, they induce dramatic transcriptional remodeling only in cancer cells.

Lower concentration MTZ and 8-OAc activate UPR^{MT} in worms but fail to extend lifespan

Next, to determine the impact of these compounds on mitochondrial function and organismal health in vivo, we moved into a *C. elegans* model system, particularly because UPR^{MT}-mediated mitohormesis and impacts on longevity are well characterized in worms [10]. Here, we exposed wild-type *C. elegans* to our compounds by supplementing nematode growth medium (NGM) with varying concentrations. We found that all three compounds do not
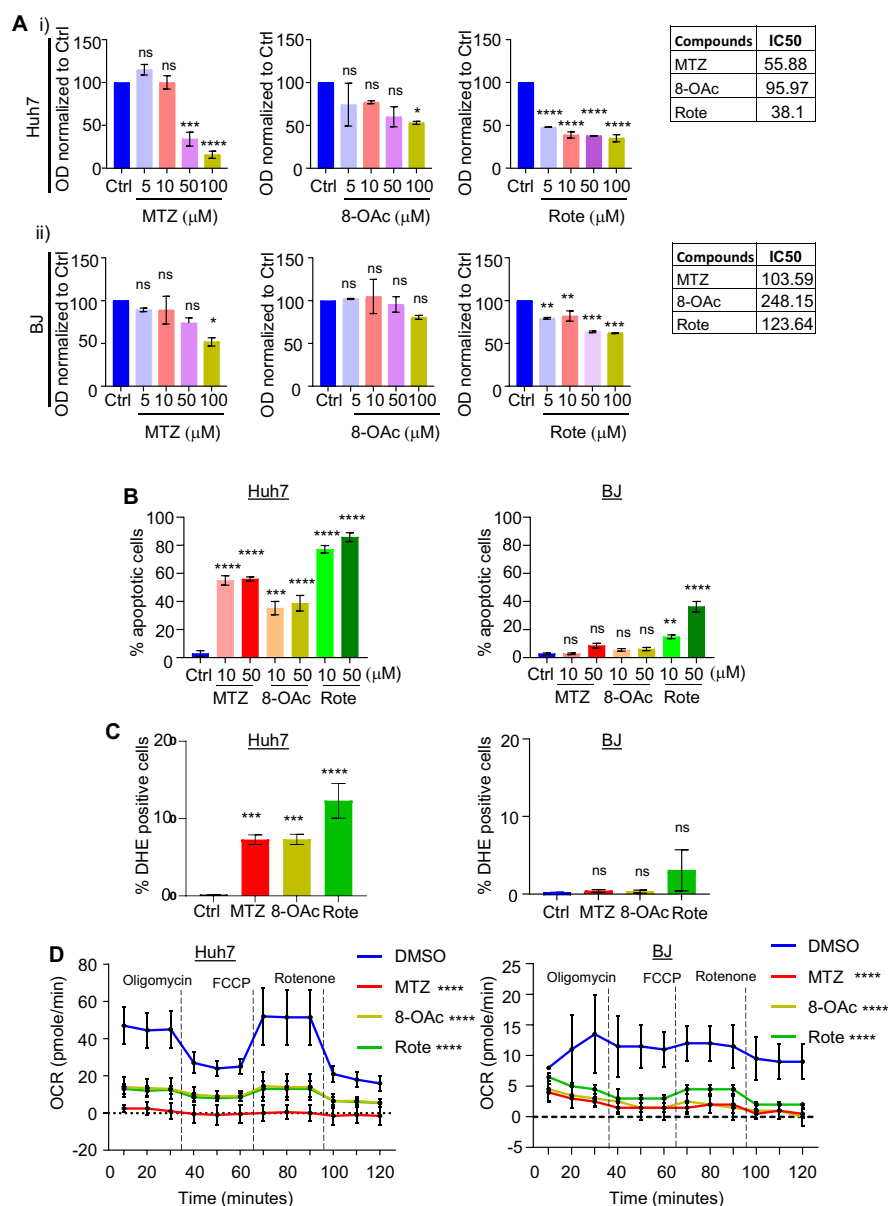
Fig. 1 Cancer cells are more sensitive than non-cancer cells to mitochondrial complex I inhibitor MTZ and 8-OAc. (**A**) Cytotoxicity of (i) Huh-7 liver carcinoma cells and (ii) BJ fibroblast non-cancer cells by MTT assay after treatment with vehicle/DMSO or various concentrations of MTZ, 8-OAc, and Rote treatment for 24h. Data is presented as OD values normalized to the DMSO-treated control. Corresponding chart shows the IC50 values of cells. (**B**) Bar graphs represent the percentage of early apoptotic cells analyzed by flow cytometry with annexin V and propidium iodide double staining after treatment with DMSO or indicated concentration of MTZ, 8-OAc, and Rote for 24h. (**C**) Graphs show the percentage of ROS-producing cells analyzed by flow cytometry with DHE staining after treating Huh-7 and BJ with DMSO or MTZ, 8-OAc, and Rote for 24h. (**D**) Graphs showing the inhibition of oxygen consumption rate after treating the indicated cells with 10μM of MTZ, 8-OAc, or Rote for 24h in comparison with vehicle control DMSO. Bar graphs represent mean and standard deviation. All statistical analysis was performed by one-way ANOVA using GraphPad Prism 10. ns = not significant, * = $p < 0.03$; ** = $p < 0.002$; *** = $p < 0.0002$; **** = $p < 0.0001$

impact development if animals are exposed to up to 3 μM concentrations from the 1st larval stage (L1). However, concentrations above 3 μM resulted in a developmental delay, with MTZ and Rote having more profound effects than 8-OAc (Fig. 2A). Since previous studies have shown that UPR^{MT}-mediated mitohormesis generally involves early-life exposure to ETC inhibition during development [32, 33], we opted for 1 and 3 μM concentrations that allowed us to expose worms to these compounds throughout development. To first confirm that these compounds inhibited mitochondrial function in vivo, we again measured mitochondrial respiration rates using Seahorse assay. Interestingly, we found that although all three compounds significantly reduced oxygen consumption rates at 3 μM concentrations, only MTZ was sufficient to reduce respiration at the lower concentration of 1 μM (Fig. 2B). These data suggest that in *C. elegans*, MTZ has a more profound effect on mitochondrial respiration compared to 8-OAc and Rote.

Considering the established association of mitochondrial ETC inhibition and activation of the UPR^{MT}, we next assessed the impact of MTZ and 8-OAc on the UPR^{MT} using the *hsp-6p::GFP* reporter [34] (Fig. 2C). We found that all three compounds induced UPR^{MT} activation at both the 1 and 3 μM concentrations (Fig. 2D). Importantly, this induction of UPR^{MT} required ATFS-1, the canonical transcription factor involved in UPR^{MT} activation [35], as RNAi knockdown of *atfs-1* completely suppressed the UPR^{MT} induction upon compound treatment (Fig. s5A). We found that all three compounds also increased expression and nuclear localization of DVE-1::GFP, another robust reporter for UPR^{MT} activation (Fig. s5B) [36]. Interestingly, all three compounds had profoundly different impacts on mitochondrial morphology in *C. elegans* (Fig. s6). Specifically, we found that all three compounds caused fragmentation of mitochondria in the muscle, but only MTZ caused fragmentation of mitochondria in the intestine at both concentrations. Rote only induced mitochondrial fragmentation in the intestine at the 3 μM concentration, whereas 8-OAc failed to induce mitochondrial fragmentation at either concentration. Finally, 8-OAc induced mitochondrial fragmentation in the hypodermis at both concentrations, whereas MTZ only induced mitochondrial fragmentation in the hypodermis at the 3 μM concentration and

Rote failed to induce mitochondrial fragmentation at either concentration in the hypodermis. These data suggest that while all three compounds impact mitochondrial ETC function and induce the UPR^{MT}, they display some differences in their downstream effects and may even have cell-type specific effects. Finally, to determine whether the inhibition of ETC and activation of UPR^{MT} was sufficient to drive mitohormesis and lifespan extension, we next measured lifespan of animals exposed to 1 and 3 μM concentration of the compounds from L1. Surprisingly, we did not observe any measurable increase in lifespan at either concentration for any of the compounds (Fig. 2E), suggesting that although UPR^{MT} is activated, it is not sufficient to drive mitohormesis.

Higher concentration of MTZ and 8-OAc extend lifespan of adult worms

The absence of lifespan changes of worms at lower concentration of MTZ and 8-OAc led us to question whether higher concentrations of these compounds could potentially impact longevity. However, it is notable that we observed a developmental defect in worms when exposed to a concentration exceeding 3 μM beginning from the L1 stage (Fig. 2A). Therefore, to expose worms to higher concentrations of compounds, we opted to expose animals to plates containing 5 μM concentration of compounds at the beginning of day 1 of adulthood (Fig. 3A). Importantly, exposing animals to 5 μM concentration of these compounds at the day 1 adult stage was still sufficient to significantly reduce mitochondrial respiration rate (Fig. 3B). Exposure of animals to this higher concentration of compounds was sufficient to drive lifespan extension (Fig. 3C). To our surprise, we did not observe an induction of UPR^{MT} activity using the *hsp-6p::GFP* reporter (Fig. 3D) or DVE-1::GFP reporter (Fig. s7A). While these data may suggest that the lifespan extension is not through UPR^{MT}-mediated mitohormesis, it is important to recognize that while the *hsp-6p::GFP* reporter is a robust method that allows for quickly testing for activation of UPR^{MT}, it is a single-gene reporter and cannot entirely encompass the UPR^{MT} activation.

Therefore, we performed a transcriptomic analysis by RNA-seq to more widely assess activation of the UPR^{MT}. We found that MTZ treatment resulted in more widespread changes in transcriptome, while
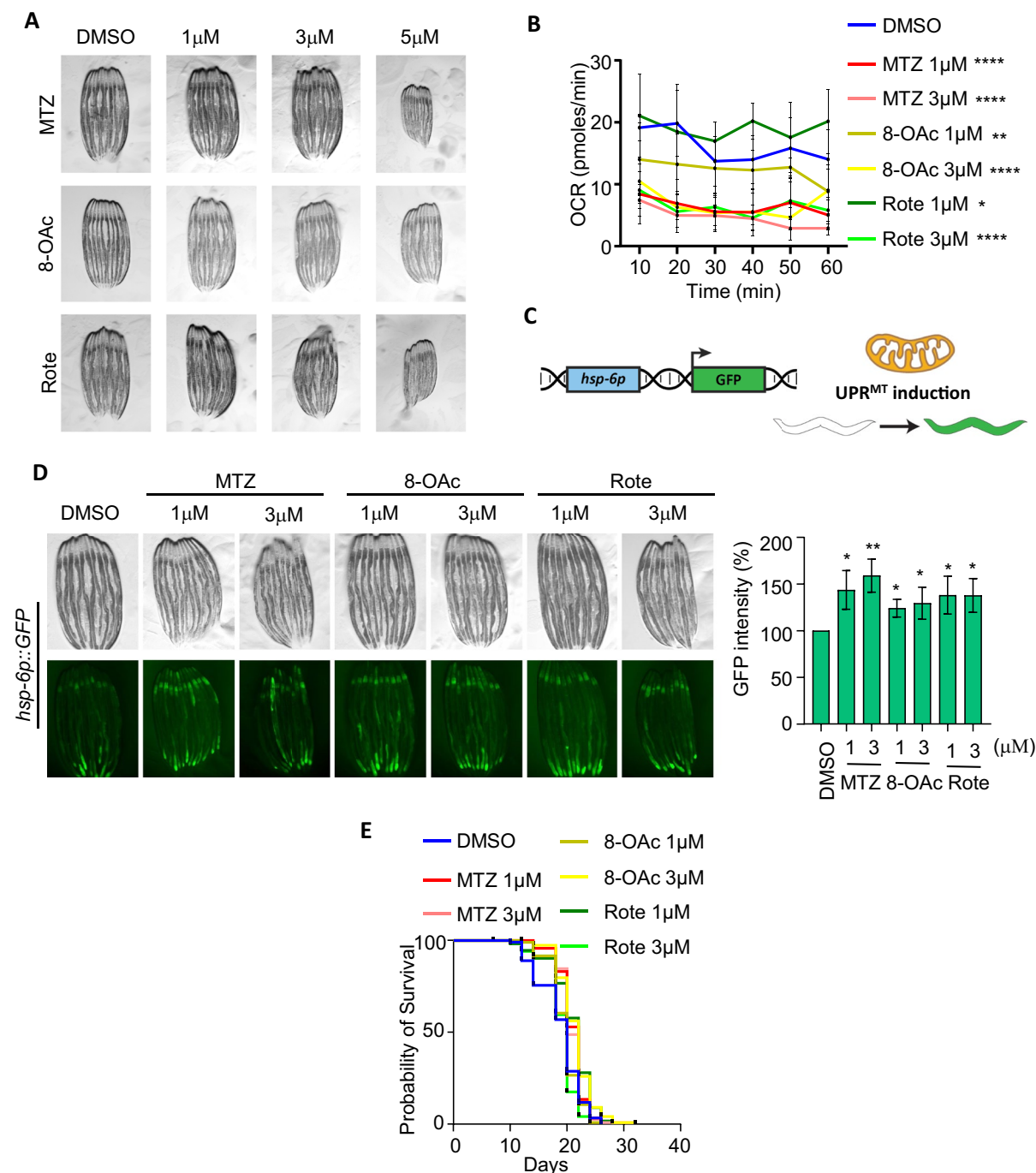
8-OAc had the smallest effect (Fig. 4A-B). Importantly, genes related to UPR^MT showed significant changes for all three compounds, which confirms that they induce UPR^MT, despite the lack of *hsp-6p::GFP* reporter induction (Fig. 4C-D). In addition, we did not see major changes in other stress response pathways including the unfolded protein response of the endoplasmic reticulum (UPR^ER) or the heat-shock response (HSR) (Fig. 3D). These data were confirmed using reporters for the HSR (*hsp-16.2p::GFP*) and the UPR^ER (*hsp-4p::GFP*), both of which showed no induction upon treatment with MTZ, 8-OAc, or Rote

◀**Fig. 2** Low concentration of MTZ and 8-OAc activate UPR^MT, but do not impact lifespan. (**A**) Representative images of wild-type N2 animals grown on DMSO controls or the indicated concentrations of MTZ, 8-OAc, or Rote from L1 for 3 days at 20 °C (i.e., day 1 adulthood for control conditions). (**B**) Seahorse analysis of mitochondrial respiration/OCR (pmol/min) of day 1 adult wild-type worms after growing them on indicated concentration of MTZ, 8-OAc or Rote from L1 until day 1 of adulthood. (**C**) Schematic representation of UPR^MT transcriptional reporter, *hsp-6p::GFP*. (**D**) Representative fluorescent micrograph of UPR^MT transcriptional reporter worms (*hsp-6p::GFP*) of day 1 adult wild-type animals grown on specified concentration of MTZ, 8-OAc, or Rote from L1. The corresponding bar graph shows the graphical representation of change in GFP intensity of the worms treated with indicated concentration of MTZ, 8-OAc or Rote compared to the control DMSO. Statistical analysis was performed by one-way ANOVA using GraphPad Prism 10. ns = not significant, * = $p < 0.03$; ** = $p < 0.002$; *** = $p < 0.0002$; **** = $p < 0.0001$ (**E**) Survival of wild-type N2 animals grown on DMSO control or indicated concentrations of MTZ, 8-OAc, or Rote from L1

(Fig. s7B-C). GO analysis of differentially expressed genes revealed many groups of genes that are consistent with a role for inhibition of mitochondrial function and mitohormesis pathways downstream of ETC dysfunction, including those involved in ETC function, response to reactive oxygen species, and mitochondrial transporter (Fig. 4E). Altogether, our transcriptomic analysis revealed that as expected, all three compounds induce UPR^MT pathways without affecting other stress response pathways.

To directly test whether the lifespan extension observed after treatment with each compound is dependent on UPR^MT pathways, we performed lifespan experiments on animals with *atfs-1* knockdown where UPR^MT activation is suppressed. Interestingly, we found dramatic differences in the effect of all three compounds upon *atfs-1* knockdown. Specifically, MTZ and Rote treatment resulted in a decrease in lifespan with MTZ having more profound effects, suggesting that in the absence of a beneficial UPR^MT activation, not only do MTZ and Rote fail to extend lifespan, but they become toxic to worms. To our surprise, we found that the lifespan extension of 8-OAc is independent of *atfs-1* (Fig. 5A). Previous studies have revealed that the heat-shock transcription factor, HSF-1, is also required for activation of UPR^MT [37]. Therefore, we also tested the requirement of HSF-1 on lifespan extension and found that RNAi knockdown of *hsf-1* suppressed the lifespan extension found upon treatment by MTZ, 8-OAc, and Rote

(Fig. 5B). Interestingly, similar to the loss of *atfs-1*, MTZ displayed a shortening of lifespan upon *hsf-1* knockdown, suggesting that in the context of *hsf-1* loss, MTZ is toxic.

Finally, since HSF1 is also involved in oxidative stress response [38] we measured the activation of oxidative stress response pathway in response to MTZ, 8-OAc, or Rote treatment using *gst-4P::GFP* reporter worms. Interestingly, we did not find any significant increase in oxidative stress response using this reporter, except for a minor increase in Rote-treated animals (Fig. s7D). However, similar to UPR^MT, it is important to understand the limitation of using reporter strains as it only measures expression of a single gene. Thus, we further evaluated oxidative stress response-related genes in our RNA-seq data and found that 8-OAc resulted in changes in expression of antioxidant genes (sTable 1). Therefore, we sought to determine whether the lifespan extension found upon treatment with MTZ, 8-OAc, or Rote were dependent upon activation of antioxidant defense pathways. We silenced *daf-16*, a crucial gene associated with the oxidative stress response pathway but did not observe any involvement of *daf-16* in the extension of lifespan under compound treatment (Fig. 5C). To further investigate the effect of redox homeostasis on longevity, we performed lifespan experiments after quenching reactive oxygen species (ROS) within cells by using N-acetylcysteine (NAC) and observed that NAC suppressed the lifespan extension of both MTZ and 8-OAc treatment but did not affect the lifespan extension of Rote treatment (Fig. 5D). These data suggest that at least in the case of MTZ and 8-OAc, the synthesis of ROS, and likely the activation of downstream detoxification pathways is involved in the longevity found upon treatment with these compounds.

Discussion

Gene level manipulation such as gene knockout or knockdown is a highly robust approach for studying the effect of a protein's function in specific cellular events [39]. However, these methods show several substantial limitations. First, animals with constitutive gene knockouts – especially for those knockouts that cause dramatic physiological changes – can pick up suppressors or adaptations, which can mask
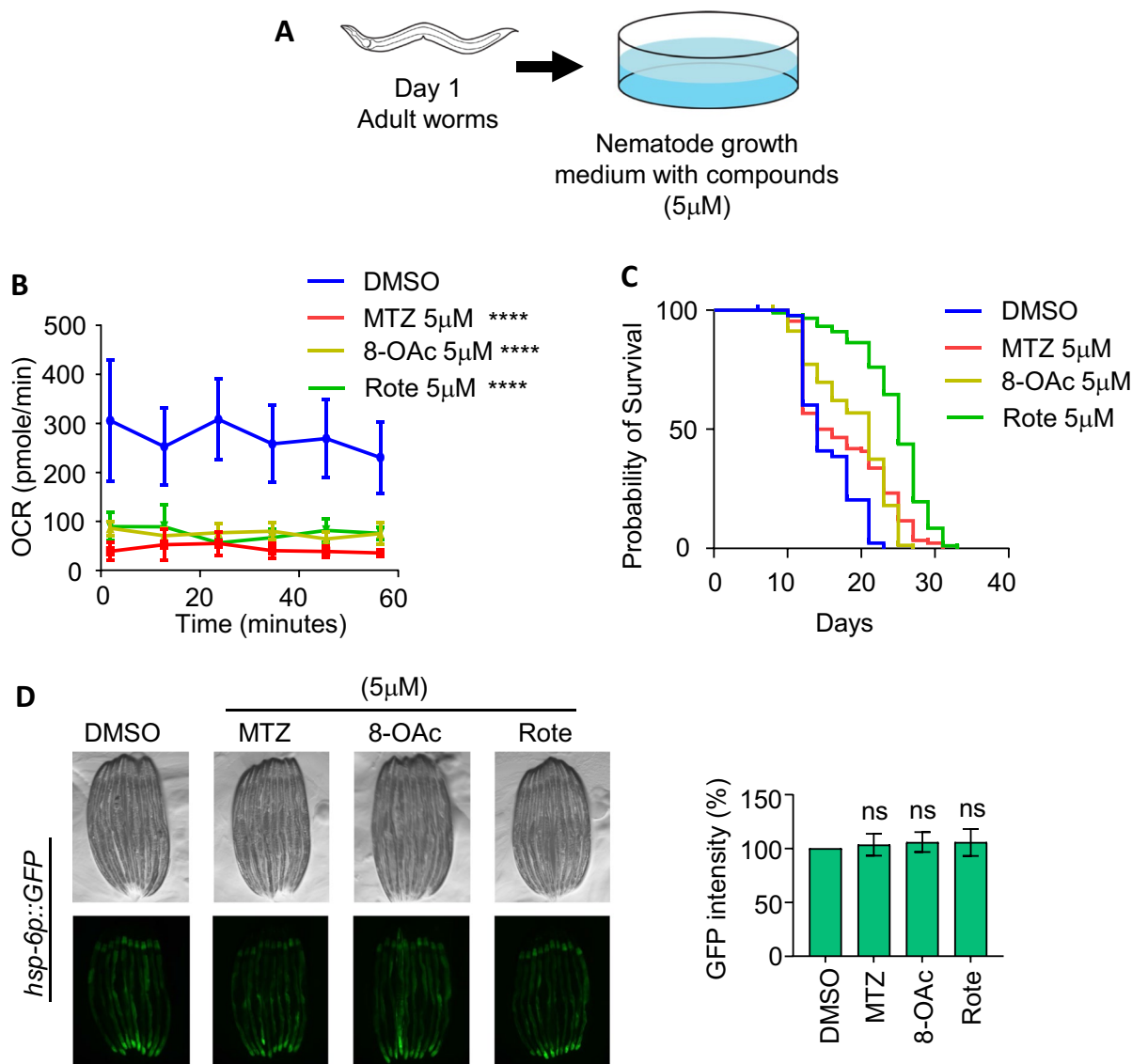
Fig. 3 High concentrations of MTZ and 8-OAc promotes longevity. (**A**) Schematic of worms treated with high concentrations of compounds starting from day 1 of adulthood. (**B**) Seahorse analysis of mitochondrial respiration/OCR (pmol/min) of day 2 adult wild-type worms after growing them on 5 μM MTZ, 8-OAc, and Rote for 24 hours starting from day 1 of adulthood. (**C**) Survival of wild-type N2 animals grown on DMSO control or 5 μM MTZ, 8-OAc, or Rote from day 1 of adulthood. (**D**) Representative fluorescent micrograph of UPR^{MT} transcriptional reporter worms (*hsp-6p::GFP*) of day 2 adult animals grown on 5 μM MTZ, 8-OAc, or Rote for 24 h from day 1 of adulthood. The corresponding bar graph shows the graphical representation of change in GFP intensity of the worms treated with indicated concentration of MTZ, 8-OAc or Rote compared to the control DMSO. Statistical analysis was performed by one-way ANOVA using GraphPad Prism 10. ns = not significant, * = $p < 0.03$; ** = $p < 0.002$; *** = $p < 0.0002$; **** = $p < 0.0001$

important phenotypes. Moreover, with certain strategies for knockdown or knockout, there are potential off-target effects, which can cause consequences from unintended genetic alterations [40, 41]. Finally, the most prominent limitation may be in the challenge of

performing genetic manipulations in highly complex systems, such as long-lived vertebrate systems or in human biology [42]. In this context, small molecule chemical probe inhibitors, particularly those isolated from natural sources, offer distinct advantages over
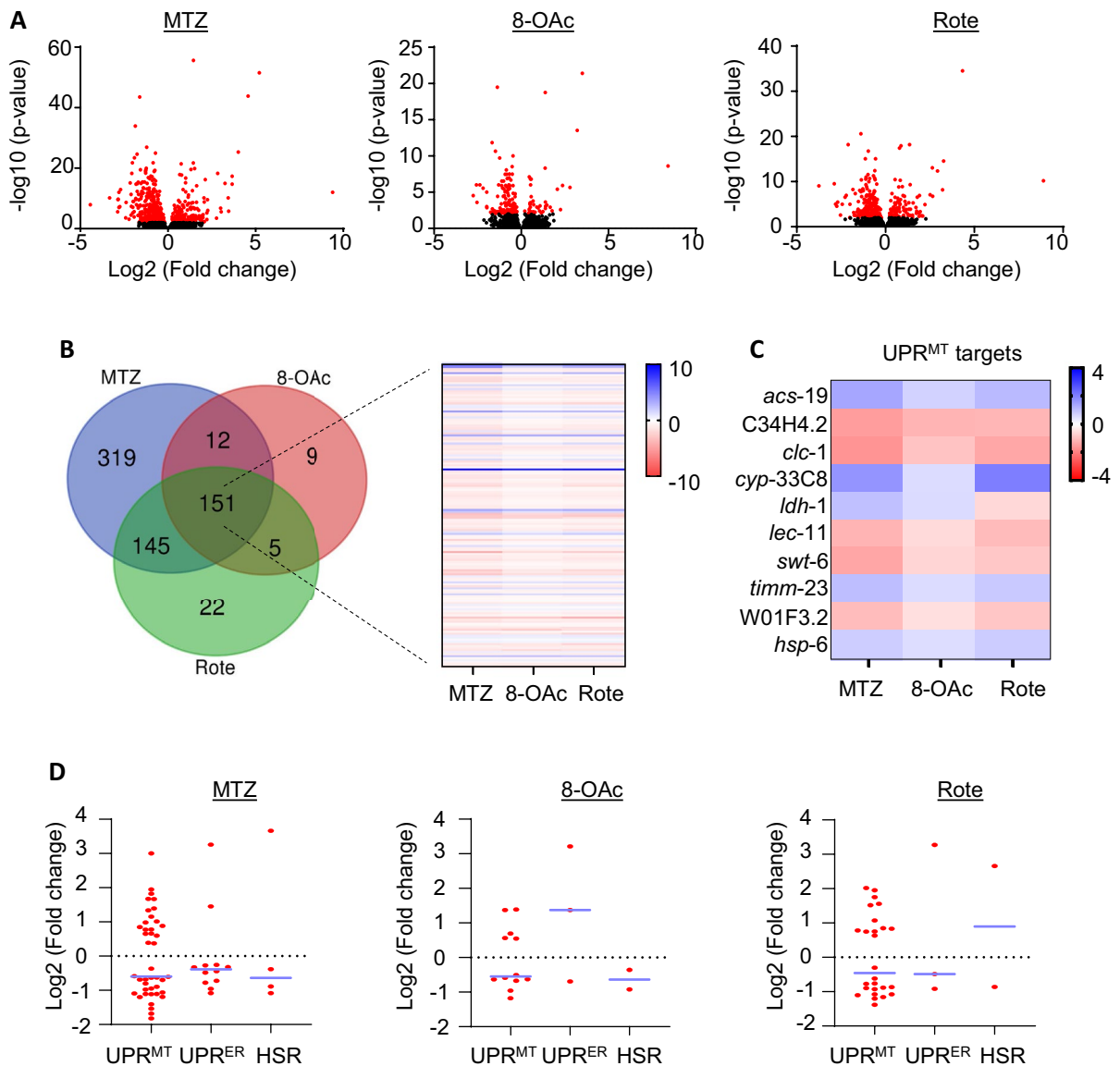
Fig. 4 Transcriptomics analysis of MTZ, 8-OAc, and Rote. (**A**) Volcano plots representing the changes in gene expression in MTZ, 8-OAc, or Rote treated worms. For RNA-seq analysis, sterile *glp-4(bn2)* animals were grown at 22 °C until day 1 of adulthood and animals were moved onto compounds at day 1 and RNA was collected at day 2 of adulthood after 24 h of growth on compounds. Data was analyzed on 3 biological replicates for each condition. Red dots indicate significantly differentially expressed genes, while black dots indicate genes that are not significant. (**B**) Venn diagram representing the overlap of significant differentially expressed genes in indicated treatment conditions. Heatmap represents the expression profile of common genes for indicated treatment conditions. (**C**) Heatmap showing the expression profile of UPR^MT target genes found common for MTZ, 8-OAc, or Rote treated conditions. (**D**) Representative graphs indicating the change in the gene expression of the indicated gene groups in MTZ, 8-OAc, or Rote treated condition as compared with DMSO control. Each dot represents a single gene and lines are median and interquartile range

gene manipulation approaches [43]. They often offer high specificity in their mode of action, thus showing more reliability to target a particular protein or any specific cellular pathway. Importantly, they also provide temporal control for reversable modulation of a protein function. Finally, these chemical probes

Fig. 5 Lifespan extension of MTZ, 8-OAc, and Rote utilize different mechanisms. (**A**) Survival of wild-type N2 animals grown on *atfs-1* RNAi on DMSO control or 5 μM MTZ, 8-OAc, or Rote from day 1 of adulthood. (**B**) Survival of wild-type N2 animals grown on *hsf-1* RNAi on DMSO control or 5 μM MTZ, 8-OAc, or Rote from day 1 of adulthood. (**C**) Survival of wild-type N2 animals grown on *daf-16* RNAi on DMSO control or 5 μM MTZ, 8-OAc, or Rote from day 1 of adulthood. (**D**) Survival of wild-type N2 animals grown on NAC-supplemented plates containing DMSO control or 5 μM MTZ, 8-OAc, or Rote from day 1 of adulthood. (**E**) Graphical description of MTZ and 8-OAc as novel compounds used to inhibit complex I and promote mitohormesis, potentially through the activation of ATFS-1 and HSF1
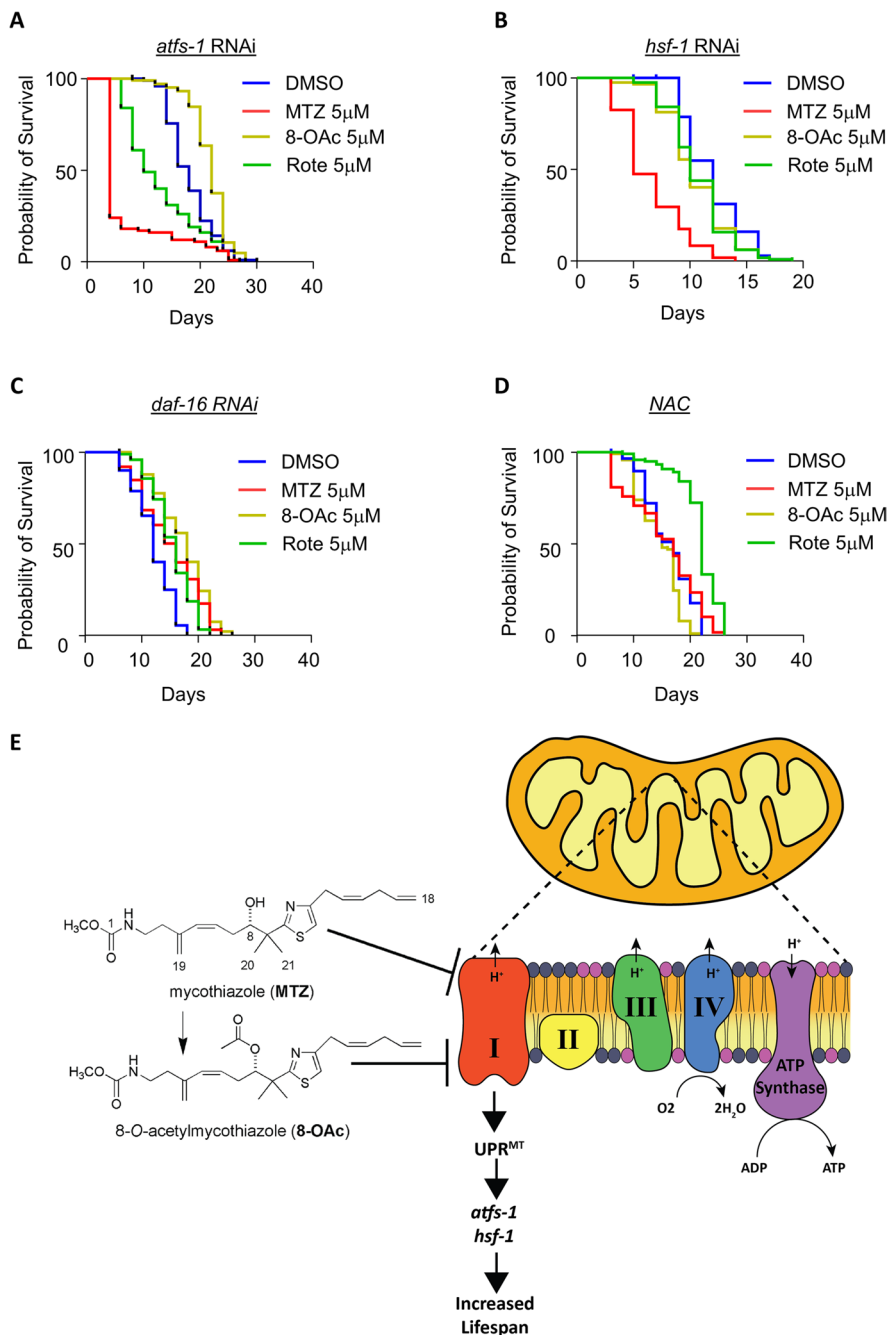
can be utilized in most model systems and in humans without the need for any genetic manipulations or interventions. As such, small molecule inhibitors have become a valuable source for therapeutic drug discovery [44]. Modification in the structure of a known or previously characterized small molecule is also common practice in the field of drug discovery research to obtain new therapeutics with better pharmacological efficiency. Chemical modifications can improve the bioavailability of a small molecule through enhancing its permeability, absorption, distribution, and regulation of its excretion properties which in turn enhance the half-life of that molecule in the body. Alteration in the structure of a small molecule based on the

knowledge of its target site can also increase the specificity of that molecule with its receptor, which can selectively reduce the off-target effects of that molecule. Modifications can also be done to provide more stability to the lead compound in diverse physiological conditions without hampering its basic properties [45–47].

In this study, we focused on compounds that target mitochondrial function. As an organelle involved in many important cellular processes including energy homeostasis, cellular metabolism, and programmed cell death, it is often a key target for the development of new therapeutics in drug development research. Mitochondrial function can be disrupted in various ways, including inhibition of different components of the ETC. Usually compounds that disrupt mitochondrial function result in toxic consequences like uncontrolled production of reactive oxygen species, which can induce cell death and lead to serious consequences including drug-induced liver injury and cardiotoxicity in humans [48, 49]. Alternatively, there are several mitochondrial inhibitors such as metformin, nitric oxide, and arsenic trioxide, that are commonly studied in the clinic for potentially beneficial effects [50]. Atovaquone, a specific inhibitor for ETC complex III also showed very promising anti-cancer activity in patients [51]. OPB-51602, a specific ETC complex I inhibitor displayed significant tumor regression in patients with secondary resistance to epidermal growth factor receptor inhibitors in a phase 1 clinical trial [52]. The clinical utility of these inhibitors also extends beyond their anti-proliferative properties. Some potent ETC inhibitors such as the complex I inhibitor papaverine are used to reduce cellular oxygen consumption, which resulted in improved radiosensitivity to solid malignancies through tumor reoxygenation [53]. However, it is noteworthy that the clinical trials of certain ETC inhibitors such as BAY87-2243, ASP4132, IACS-010759 were terminated due to their dose limiting toxicities [54–56]. Thus, the study of additional mitochondrial inhibitors can be a valuable source for drug discovery.

Rote is another extensively studied molecule that inhibits the ETC, specifically complex I. It is mainly used as a pesticide in agriculture and aquaculture, but its use has raised major concern because of its off-target effects on other species in the agricultural field and aquatic ecosystem [57]. In human biology, it exhibits promising anticancer properties [57], but in our study,

we found that it showed significant toxicity to non-cancer cells. Previous studies have shown that MTZ and 8-OAc similarly exhibit significant activity against a wide range of cancer cell types [21]. In our study, we confirmed these findings although we noticed a difference in functional concentration of MTZ and 8-OAc compared to the previous study. In our attempt to replicate their findings, we titrated lower concentrations of these small molecules as reported previously. Surprisingly, at these lower concentrations, we did not observe any biological effects, including cytotoxicity, changes in OCR, or alterations in mitochondrial morphology. Instead, we found that the biological effects of these small molecules manifested in the micromolar range. This observation was intriguing; although the effective concentrations are higher than previously reported, it is not entirely unexpected given the variability in small molecule responses under different conditions. Changes in environmental factors during the isolation process, such as temperature or pressure, transitions between physical states, solubility and variations in cell culture conditions, including pH, ionic strength, and composition of culture media all can influence the effective concentration of a small molecule. More importantly, we show that both MTZ and 8-OAc can induce ROS production, leading to cell death in liver cancer cells. While all three compounds displayed higher toxicity to the specific cancer cells in this study (liver carcinoma, breast cancer, and glioblastoma), 8-OAc specifically exhibited negligible toxicity against non-cancer cell types at a concentration where Rote and MTZ showed mild toxicity, suggesting this class has potential therapeutic utility based on its unique selectivity to kill cancer cells.

We also found that all three compounds directly inhibited mitochondrial function in both cancer and non-cancer cell lines as measured by reduced oxygen consumption rate. However, these compounds only resulted in mitochondrial fragmentation in cancer cells and not non-cancer cells. Our data uncouples the effects of mitochondrial respiration on mitochondrial morphology and dynamics, at least in the case of cultured cells. It is important to acknowledge recent limitations observed in the field of mitochondrial research related to cell culture experiments. The rigid polystyrene substrate used in tissue culture plates can elevate mechanosignaling pathways in cells through activation of HSF1 [58]. Similarly, growth in high glucose conditions can

also elevate HSF1 signaling and alter mitochondrial metabolism [59]. Indeed, we found that BJ fibroblasts grown on polystyrene and high glucose conditions exhibited negligible response to the standard mitochondrial respiration-inhibiting compounds (oligomycin, FCCP, and Rote) during the Seahorse assay, which potentially suggests that OCR in these cells may not be dependent on mitochondrial respiration. However, it is important to note that in the Seahorse assay, these compounds are added minutes before taking OCR measurements, so it is entirely possible that BJ fibroblasts simply respond slower to mitochondrial respiration-inhibiting drugs. This would be consistent with our findings that 24-hour Rote treatment does indeed reduce OCR significantly. Regardless, these limitations to our study are very important to keep in mind as it is possible that the effects we see in non-cancer cells may be obscured by the usage of both high glucose medium and growth on polystyrene. Further investigation is necessary to explore the specificity of these compounds on cancer cells in an in vivo system or organoid system that circumvents these issues.

Going forward, we opted to complement our cell culture system using the in vivo *C. elegans* model system. While *C. elegans* do not allow for cancer studies, they are an excellent model system for understanding the effects of mitochondrial inhibition on aging, particularly as a commonly used model for mitohormesis pathways [60]. At first, we opted to use 1 and 3 μM concentrations of MTZ and 8-OAc due to developmental delays in worms exposed to higher concentrations of compounds. We opted for lower concentrations as numerous mitohormesis studies have shown the importance of exposure to mitochondrial stress during development, which would not have been possible at the concentrations that induced developmental defects. Shockingly, while we saw UPR^{MT} activation at these lower concentrations, there was no lifespan extension. Instead, we observed a significant lifespan extension when animals were exposed to these compounds at higher concentrations post-development. Several studies have shown that lifespan extension via mitohormesis through ETC inhibition require inhibition during development [32, 33]. In addition, RNAi of various ETC complex subunits fail to extend lifespan in worms if applied in their adulthood. Notably, post-developmental inhibition of *atp*-3 can cause a remarkable induction in UPR^{MT} but

shorten lifespan [61]. In contrast, our studies indicate that activation of a beneficial mitohormesis occurs after adulthood when ETC inhibition occurs via compounds. While it is entirely possible that this is due to different effects of compounds versus genetic intervention via RNAi, they highlight how mitohormesis via ETC inhibition are context dependent. A major limitation to our study to address this concern is that treatment with high concentrations of MTZ, 8OAc, or Rote results in developmental defects. Therefore, we unfortunately cannot make direct comparisons between the genetic interventions previously performed with our chemical compound studies here due to experimental differences.

Interestingly, we did not observe activation of *hsp-6p::GFP* in animals exposed to high concentrations of MTZ, 8-OAc, or Rote, despite these animals exhibiting extended lifespans. These data complement studies that have shown that *hsp-6p::GFP* expression is not always correlated with lifespan extension in mitohormesis pathways [62]. However, more comprehensive transcriptome analysis using RNA-seq did indeed show that exposure to all three compounds induced genes associated with canonical UPR^{MT}, which highlight the fact that a single-gene reporter, while useful for preliminary analyses, cannot be used as final conclusive evidence for stress responses. Another interesting phenomenon we observed from our RNA-seq analysis was that 8-OAc displayed the least number of differentially expressed genes both in human cells and in *C. elegans* in comparison to MTZ and Rote. We hypothesize that this is potentially due to 8-OAc having a more specific effect on mitochondrial ETC function with less off-target effects. Indeed, genes differentially expressed under 8-OAc conditions are more related to inhibition of mitochondrial function including antioxidant defense pathways, while MTZ and Rote induced gene expression changes in a diverse array of seemingly unrelated pathways including defense response to bacterium, translational elongation process, sodium ion export from cell, cell morphogenesis, etc. (sTable 2). It is possible that the increased stability of 8-OAc compared to MTZ can be partially responsible for these effects, as we have also observed that old (>6 mos.) – and likely partially degraded – MTZ [21] can have toxic effects on *C. elegans* and cause premature death in animals. These findings highlight the importance of medicinal chemistry modifications to lead compounds for structural

optimization to augment their chemical stability (shelf life) while maintaining their potency and selectivity required for specific modes of action.

Finally, one of our most interesting findings was the observation that MTZ, and 8-OAc utilized distinct downstream mechanisms to promote longevity in *C. elegans* (Fig. 5E). While the lifespan extension by MTZ was dependent on *atfs-1* and *hsf-1*, 8-OAc is only dependent on *hsf-1*. Numerous studies have implicated HSF1 in mitochondrial stress response: William *et. al.* has shown in *C. elegans* that in response to ETC impairment, a mitochondria specific variant of HSF1 is activated by a specific dephosphorylation event, which results in the induction of specific heat shock proteins [63]. Furthermore, another study in mammalian cells showed that HSF1 constitutively binds with the promoters of mitochondrial chaperones. In response to mitochondrial stress that occupancy remarkably enhanced and induces the production of mitochondrial chaperones [37]. Finally, mitochondrial stress can prevent proteostasis collapse during aging by improving HSF1 function at late age [63]. Our observations align with these previous studies highlighting the overlap of mitohormesis and HSF1, and its implications on aging. Still to be understood is whether the beneficial effects of HSF1 in the context of MTZ and 8-OAc is through canonical UPR^{MT} pathways or some other function of HSF1. Considering the lack of canonical HSR genes identified in our RNA-seq pathway, it is likely that the lifespan extension of MTZ is not through canonical HSR, but potentially through an ATFS-1/HSF1 dependent activation of UPR^{MT}. In the case of 8-OAc, it is possible that both HSF1-mediated UPR^{MT} and HSF1 driven antioxidant pathways may be involved in lifespan extension, as our RNA-seq revealed induction of several antioxidant pathways and NAC treatment suppressed lifespan extension in 8-OAc treated conditions. However, this is just one of many potential possibilities and further experiments are required to make conclusive statements. Overall, these findings underscore the complexity of UPR^{MT} regulation and its intricate collaboration with other stress response pathways and advocate for further in-depth exploration. Most importantly, as a cautionary tale, our study highlights the critical importance of testing multiple compounds of the same chemotype as similar structures with seemingly identical effects may have some important differences on biological mechanisms of action.

In summary, this comprehensive study elucidates the efficacy of two highly potent and selective small molecule inhibitors of the ETC, MTZ and 8-OAc in cancer and aging studies. These compounds hold promise as effective alternatives to existing small molecule inhibitor chemical probes, such as Rote, offering new insights in the domains of mitochondrial and aging-related research. The remarkable lack of off-target effects and higher stability of 8-OAc highlights the significance of how minor semisynthetic modifications to natural products can optimize the structure of lead compounds to provide improved stability, retained potency and selectivity. Ultimately the structure of 8-OAc is poised to serve as a promising next generation chemical probe to accelerate the study of mitochondrial dynamics in chemical biology to potentially offer new avenues for the development of anti-cancer and anti-aging therapeutics.

Data availability All data required to evaluate the conclusions in this manuscript are available within the manuscript and Supporting Information. All strains synthesized in this manuscript are derivatives of N2 or other strains from CGC and are either made available on CGC or available upon request. All raw RNA-seq datasets are available through Annotare 2.0 Array Express Accession E-MTAB-13546.

Declarations

Competing interests All authors of the manuscript declare that they have no competing interests.

References

1. Casanova A, Wevers A, Navarro-Ledesma S, Pruimboom L. Mitochondria: It is all about energy. Front Physiol. 2023;14(April):1114231. https://doi.org/10.3389/fphys.2023.1114231.
2. Chen Y, Zhou Z, Min W. Mitochondria, oxidative stress and innate immunity. Front Physiol. 2018;9(October):1487. https://doi.org/10.3389/fphys.2018.01487.
3. Shen K, Pender CL, Bar-Ziv R, Zhang H, Wickham K, Willey E, Durieux J, Ahmad Q, Dillin A. Mitochondria as cellular and organismal signaling hubs. Annu Rev Cell Dev Biol. 2022;38(1):179–218. https://doi.org/10.1146/annurev-cellbio-120420-015303.
4. Green DR. The mitochondrial pathway of apoptosis: Part I: Momp and beyond. Cold Spring Harb Perspect Biol. 2022;14(5):a041038. https://doi.org/10.1101/cshperspect.a041038.
5. Bar-Ziv R, Bolas T, Dillin A. Systemic effects of mitochondrial stress. EMBO Rep. 2020a;21(6):e50094. https://doi.org/10.15252/embr.202050094.
6. Amorim JA, Coppotelli G, Rolo AP, Palmeira CM, Ross JM, Sinclair DA. Mitochondrial and metabolic dysfunction in ageing and age-related diseases. Nat Rev Endocrinol. 2022;18(4):243–58. https://doi.org/10.1038/s41574-021-00626-7.
7. López-Otín C, Blasco MA, Partridge L, Serrano M, Kroemer G. Hallmarks of aging: an expanding universe. Cell. 2023;186(2):243–78. https://doi.org/10.1016/j.cell.2022.11.001.
8. Srivastava S. The mitochondrial basis of aging and age-related disorders. Genes. 2017;8(12):398. https://doi.org/10.3390/genes8120398.
9. Ristow M, Zarse K. How increased oxidative stress promotes longevity and metabolic health: the concept of mitochondrial hormesis (mitohormesis). Exp Gerontol. 2010;45(6):410–8. https://doi.org/10.1016/j.exger.2010.03.014.
10. Dutta N, Garcia G, Higuchi-Sanabria R. Hijacking cellular stress responses to promote lifespan. Front Aging. 2022a;3(March):860404. https://doi.org/10.3389/fragi.2022.860404.
11. Owusu-Ansah E, Song W, Perrimon N. Muscle mitohormesis promotes longevity via systemic repression of insulin signaling. Cell. 2013;155(3):699–712. https://doi.org/10.1016/j.cell.2013.09.021.
12. Durieux J, Wolff S, Dillin A. The cell-non-autonomous nature of electron transport chain-mediated longevity. Cell. 2011;144(1):79–91. https://doi.org/10.1016/j.cell.2010.12.016.
13. Higuchi-Sanabria R, Frankino PA, Paul JW, Tronnes SU, Dillin A. A futile battle? Protein quality control and the stress of aging. Dev Cell. 2018;44(2):139–63. https://doi.org/10.1016/j.devcel.2017.12.020.
14. Bonkowski MS, Sinclair DA. Slowing ageing by design: The rise of NAD+ and sirtuin-activating compounds. Nat Rev Mol Cell Biol. 2016;17(11):679–90. https://doi.org/10.1038/nrm.2016.93.
15. Ma C, Xia F, Kelley SO. Mitochondrial targeting of probes and therapeutics to the powerhouse of the cell. Bioconjug Chem. 2020;31(12):2650–67. https://doi.org/10.1021/acs.bioconjchem.0c00470.
16. Arrowsmith CH, Audia JE, Austin C, Baell J, Bennett J, Blagg J, Bountra C, et al. The promise and peril of chemical probes. Nat Chem Biol. 2015;11(8):536–41. https://doi.org/10.1038/nchembio.1867.
17. Antolin AA, Workman P, Al-Lazikani B. Public resources for chemical probes: The journey so far and the road ahead. Future Med Chem. 2021;13(8):731–47. https://doi.org/10.4155/fmc-2019-0231.
18. Risinger AL, Lin D. Targeting and extending the eukaryotic druggable genome with natural products: cytoskeletal targets of natural products. Nat Prod Rep. 2020;37(5):634–52. https://doi.org/10.1039/c9np00053d.
19. Johnson TA, Milan-Lobo L, Che T, Ferwerda M, Lambu E, McIntosh NL, Li F, et al. Identification of the first marine-derived opioid receptor 'balanced' agonist with a signaling profile that resembles the endorphins. ACS Chem Neurosci. 2017;8(3):473–85. https://doi.org/10.1021/acschemneuro.6b00167.
20. Morgan JB, Mahdi F, Liu Y, Coothankandaswamy V, Jekabsons MB, Johnson TA, Sashidhara KV, Crews P, Nagle DG, Zhou Y-D. The marine sponge metabolite mycothiazole: a novel prototype mitochondrial complex i inhibitor. Bioorg Med Chem. 2010;18(16):5988–94. https://doi.org/10.1016/j.bmc.2010.06.072.

21. Johnson TA, Morris JD, Coppage DA, Cook CV, Persi LN, Ogarrio MA, Garcia TC, et al. Reinvestigation of mycothiazole reveals the penta-2,4-dien-1-ol residue imparts picomolar potency and 8 *s* configuration. ACS Med Chem Lett. 2020;11(2):108–13. https://doi.org/10.1021/acsmedchemlett.9b00302.

22. Dobin A, Davis CA, Schlesinger F, Drenkow J, Zaleski C, Jha S, Batut P, Chaisson M, Gingeras TR. STAR: Ultrafast universal RNA-seq aligner. Bioinformatics (Oxford, England). 2013;29(1):15–21. https://doi.org/10.1093/bioinformatics/bts635.

23. Liao Y, Smyth GK, Shi W. The R package rsubread is easier, faster, cheaper and better for alignment and quantification of rna sequencing reads. Nucleic Acids Res. 2019;47(8):e47–7. https://doi.org/10.1093/nar/gkz114.

24. Risso D, Ngai J, Speed TP, Dudoit S. Normalization of RNA-seq data using factor analysis of control genes or samples. Nat Biotechnol. 2014;32(9):896–902. https://doi.org/10.1038/nbt.2931.

25. Love MI, Huber W, Anders S. Moderated estimation of fold change and dispersion for RNA-seq data with deseq2. Genome Biol. 2014;15(12):550. https://doi.org/10.1186/s13059-014-0550-8.

26. Bar-Ziv R, Frakes AE, Higuchi-Sanabria R, Bolas T, Frankino PA, Gildea HK, Metcalf MG, Dillin A. Measurements of physiological stress responses in C. *elegans*. J Vis Exp. 2020b;159(May):61001. https://doi.org/10.3791/61001.

27. Torres C, Toni DM, Averbukh M, Coakley AJ, Dutta N, Garcia G, Higuchi-Sanabria R. Surveying low-cost methods to measure lifespan and healthspan in Caenorhabditis *elegans*. J Vis Exp. 2022;183(May):64091. https://doi.org/10.3791/64091-v.

28. Sonnenschein RN, Johnson TA, Tenney K, Valeriote FA, Crews P. A reassignment of (−)-mycothiazole and the isolation of a related diol. J Nat Prod. 2006;69(1):145–7. https://doi.org/10.1021/np0503597.

29. Morris JD, Takahashi-Ruiz L, Persi LN, Summers JC, McCauley EP, Chan PYW, Amberchan G, et al. Re-evaluation of the fijianolide/laulimalide chemotype suggests an alternate mechanism of action for C-15/C-20 analogs. ACS Omega. 2022;7(10):8824–32. https://doi.org/10.1021/acsomega.1c07146.

30. Takahashi-Ruiz L, Morris JD, Crews P, Johnson TA, Risinger AL. In vivo evaluation of (−)-zampanolide demonstrates potent and persistent antitumor efficacy when targeted to the tumor site. Molecules. 2022;27(13):4244. https://doi.org/10.3390/molecules27134244.

31. Dutta N, Pemmaraju DB, Ghosh S, Ali A, Mondal A, Majumder C, Nelson VK, et al. Alkaloid-rich fraction of ervatamia coronaria sensitizes colorectal cancer through modulating AMPK and mTOR signalling pathways. J Ethnopharmacol. 2022b;283(January):114666. https://doi.org/10.1016/j.jep.2021.114666.

32. Dillin A, Hsu A-L, Arantes-Oliveira N, Lehrer-Graiwer J, Hsin H, Fraser AG, Kamath RS, Ahringer J, Kenyon C. Rates of behavior and aging specified by mitochondrial function during development. Science. 2002;298(5602):2398–401. https://doi.org/10.1126/science.1077780.

33. Rea, Shane L, Natascia Ventura, and Thomas E Johnson. 2007. "Relationship between mitochondrial electron transport chain dysfunction, development, and life extension in Caenorhabditis *elegans*." edited by Thomas B. L Kirkwood. PLoS Biol. 5 (10): e259. https://doi.org/10.1371/journal.pbio.0050259.

34. Yoneda T, Benedetti C, Urano F, Clark SG, Harding HP, Ron D. Compartment-specific perturbation of protein handling activates genes encoding mitochondrial chaperones. J Cell Sci. 2004;117(18):4055–66. https://doi.org/10.1242/jcs.01275.

35. Nargund AM, Pellegrino MW, Fiorese CJ, Baker BM, Haynes CM. Mitochondrial import efficiency of ATFS-1 regulates mitochondrial UPR activation. Science. 2012;337(6094):587–90. https://doi.org/10.1126/science.1223560.

36. Tian Y, Garcia G, Bian Q, Steffen KK, Joe L, Wolff S, Meyer BJ, Dillin A. Mitochondrial stress induces chromatin reorganization to promote longevity and UPR Mt. Cell. 2016;165(5):1197–208. https://doi.org/10.1016/j.cell.2016.04.011.

37. Katiyar A, Fujimoto M, Tan K, Kurashima A, Srivastava P, Okada M, Takii R, Nakai A. HSF1 Is required for induction of mitochondrial chaperones during the mitochondrial unfolded protein response. FEBS Open Bio. 2020;10(6):1135–48. https://doi.org/10.1002/2211-5463.12863.

38. Himanen SV, Puustinen MC, Da Silva AJ, Vihervaara A, Sistonen L. HSFs drive transcription of distinct genes and enhancers during oxidative stress and heat shock. Nucleic Acids Res. 2022;50(11):6102–15. https://doi.org/10.1093/nar/gkac493.

39. Curtis CD, Nardulli AM. Using RNA interference to study protein function. In: McEwan IJ, editor. *The nuclear receptor superfamily*, Methods in molecular biology, vol. 505. Totowa, NJ: Humana Press; 2009. p. 187–204. https://doi.org/10.1007/978-1-60327-575-0_11.

40. Carroll D. Collateral damage: benchmarking off-target effects in genome editing. Genome Biol. 2019;20(1):114. https://doi.org/10.1186/s13059-019-1725-0.

41. Höijer I, Emmanouilidou A, Östlund R, Van Schendel R, Bozorgpana S, Tijsterman M, Feuk L, Gyllensten U, Den Hoed M, Ameur A. CRISPR-Cas9 induces large structural variants at on-target and off-target sites in vivo that segregate across generations. Nat Commun. 2022;13(1):627. https://doi.org/10.1038/s41467-022-28244-5.

42. Uddin F, Rudin CM, Sen T. CRISPR gene therapy: applications, limitations, and implications for the future. Front Oncol. 2020;10(August):1387. https://doi.org/10.3389/fonc.2020.01387.

43. Weiss WA, Taylor SS, Shokat KM. Recognizing and exploiting differences between RNAi and small-molecule inhibitors. Nat Chem Biol. 2007;3(12):739–44. https://doi.org/10.1038/nchembio1207-739.

44. Beck H, Härter M, Haß B, Schmeck C, Baerfacker L. Small molecules and their impact in drug discovery: a perspective on the occasion of the 125th anniversary of the bayer chemical research laboratory. Drug Discov Today. 2022;27(6):1560–74. https://doi.org/10.1016/j.drudis.2022.02.015.

45. Bech EM, Pedersen SL, Jensen KJ. Chemical strategies for half-life extension of biopharmaceuticals: lipidation and its alternatives. ACS Med Chem Lett. 2018;9(7):577–80. https://doi.org/10.1021/acsmedchemlett.8b00226.

46. Ma Y-S, Xin R, Yang X-L, Shi Y, Zhang D-D, Wang H-M, Wang P-Y, Liu J-B, Chu K-J, Da F. Paving the way for small-molecule drug discovery. Am J Transl Res. 2021;13(3):853–70.

47. Xiong B, Wang Y, Chen Y, Xing S, Liao Q, Chen Y, Li Q, Li W, Sun H. Strategies for structural modification of small molecules to improve blood–brain barrier penetration: a recent perspective. J Med Chem. 2021;64(18):13152–73. https://doi.org/10.1021/acs.jmedchem.1c00910.

48. Barbier-Torres L, Iruzubieta P, Fernández-Ramos D, Delgado TC, Taibo D, Guitiérrez-de-Juan V, Varela-Rey M, et al. the mitochondrial negative regulator MCJ is a therapeutic target for acetaminophen-induced liver injury. Nat Commun. 2017;8(1):2068. https://doi.org/10.1038/s41467-017-01970-x.

49. Karamanlidis G, Lee CF, Garcia-Menendez L, Kolwicz SC, Suthammarak W, Gong G, Sedensky MM, Morgan PG, Wang W, Tian R. Mitochondrial complex I deficiency increases protein acetylation and accelerates heart failure. Cell Metab. 2013;18(2):239–50. https://doi.org/10.1016/j.cmet.2013.07.002.

50. Machado ND, Heather LC, Harris AL, Higgins GS. Targeting mitochondrial oxidative phosphorylation: lessons, advantages, and opportunities. Br J Cancer. 2023;129(6):897–9. https://doi.org/10.1038/s41416-023-02394-9.

51. Xiang M, Kim H, Ho VT, Walker SR, Bar-Natan M, Anahtar M, Liu S, et al. Gene expression–based discovery of atovaquone as a STAT3 inhibitor and anticancer agent. Blood. 2016;128(14):1845–53. https://doi.org/10.1182/blood-2015-07-660506.

52. Hirpara J, Jie Qing E, Tan JKM, Wong AL, Clement M-V, Kong LR, Ohi N, et al. Metabolic reprogramming of oncogene-addicted cancer cells to OXPHOS as a mechanism of drug resistance. Redox Biol. 2019;25(July):101076. https://doi.org/10.1016/j.redox.2018.101076.

53. Benej M, Hong X, Vibhute S, Scott S, Jinghai W, Graves E, Le Q-T, et al. Papaverine and its derivatives radiosensitize solid tumors by inhibiting mitochondrial metabolism. Proc Natl Acad Sci. 2018;115(42):10756–61. https://doi.org/10.1073/pnas.1808945115.

54. Janku F, LoRusso P, Mansfield AS, Nanda R, Spira A, Wang T, Melhem-Bertrandt A, Sugg J, Ball HA. First-in-human evaluation of the novel mitochondrial complex I inhibitor ASP4132 for treatment of cancer. Investig New Drugs. 2021;39(5):1348–56. https://doi.org/10.1007/s10637-021-01112-7.

55. Xu Y, Xue D, Bankhead A, Neamati N. Why all the fuss about oxidative phosphorylation (OXPHOS)? J Med Chem. 2020;63(23):14276–307. https://doi.org/10.1021/acs.jmedchem.0c01013.

56. Yap TA, Daver N, Mahendra M, Zhang J, Kamiya-Matsuoka C, Meric-Bernstam F, Kantarjian HM, et al. Complex I inhibitor of oxidative phosphorylation in advanced solid tumors and acute myeloid leukemia: phase I trials. Nat Med. 2023;29(1):115–26. https://doi.org/10.1038/s41591-022-02103-8.

57. Heinz S, Freyberger A, Lawrenz B, Schladt L, Schmuck G, Ellinger-Ziegelbauer H. Mechanistic investigations of the mitochondrial complex I inhibitor rotenone in the context of pharmacological and safety evaluation. Sci Rep. 2017;7(1):45465. https://doi.org/10.1038/srep45465.

58. Tharp KM, Higuchi-Sanabria R, Timblin GA, Ford B, Garzon-Coral C, Schneider C, Muncie JM, et al. Adhesion-mediated mechanosignaling forces mitohormesis. Cell Metab. 2021;33(7):1322–1341.e13. https://doi.org/10.1016/j.cmet.2021.04.017.

59. Irshad Z, Xue M, Ashour A, Larkin JR, Thornalley PJ, Rabbani N. Activation of the unfolded protein response in high glucose treated endothelial cells is mediated by methylglyoxal. Sci Rep. 2019;9(1):7889. https://doi.org/10.1038/s41598-019-44358-1.

60. Chen PX, Zhang L, Chen D, Tian Y. Mitochondrial stress and aging: Lessons from C. *elegans*. Semin Cell Dev Biol. 2024;154(February):69–76. https://doi.org/10.1016/j.semcdb.2023.02.010.

61. Angeli S, Foulger A, Chamoli M, Peiris TH, Gerencser A, Shahmirzadi AA, Andersen J, Lithgow G. The mitochondrial permeability transition pore activates the mitochondrial unfolded protein response and promotes aging. eLife. 2021;10:e63453. https://doi.org/10.7554/eLife.63453.

62. Bennett CF, Kaeberlein M. The mitochondrial unfolded protein response and increased longevity: cause, consequence, or correlation? Exp Gerontol. 2014;56(August):142–6. https://doi.org/10.1016/j.exger.2014.02.002.

63. Williams R, Laskovs M, Williams RI, Mahadevan A, Labbadia J. A mitochondrial stress-specific form of HSF1 protects against age-related proteostasis collapse. Dev Cell. 2020;54(6):758–772.e5. https://doi.org/10.1016/j.devcel.2020.06.038.